

## Variation in the quantity and composition of phosphorus accumulating organisms in activated sludge driven by nitrate-nitrogen

Xiaoling Wang<sup>†</sup>, Chunyan Shi, Wenbo Pan, Hai Lu, and Xiaoyu Zhang

Key Laboratory of Songliao Aquatic Environment, Ministry of Education, Jilin Jianzhu University,  
Changchun City, Jilin Province, P. R. China

(Received 29 June 2022 • Revised 6 November 2022 • Accepted 16 November 2022)

**Abstract**—Anaerobic/anoxia sequencing batch reactor (A/ASBR) system was used to analyze the quantity and composition of each branch of phosphorus accumulating organisms (PAOs) in activated sludge under different nitrate-nitrogen ( $\text{NO}_3^-$ -N) concentrations by using real-time quantitative polymerase chain reaction (PCR) technology. The study determined whether  $\text{NO}_3^-$ -N and its concentration change were the main driving factors for the variation of the quantity and composition of each branch of PAOs. The results show that with the increase of  $\text{NO}_3^-$ -N concentration from 10 mg/L to 40 mg/L, the number of bacterial 16S rRNA genes in the A/ASBR reactor changed slightly at  $6.81 \times 10^{11}$ – $7.53 \times 10^{11}$  copies/g dry sludge. The number of PAO genes (Acc 16S rRNA) increased from  $1.98 \times 10^{11}$  to  $3.53 \times 10^{11}$  copies/g dry sludge, and the total number of ppk1 genes increased from  $1.25 \times 10^{11}$  to  $3.59 \times 10^{11}$  copies/g dry sludge. Additionally, the number of polyphosphate kinase (ppk) genes in Accumulibacter branch IA, IIC and IID was high, and the changes were positively related to the concentration of  $\text{NO}_3^-$ -N, while the number of branches in IIA, IIB and IIF was very low. The dosing concentration of  $\text{NO}_3^-$ -N was the main driving factor for the change of PAOs and their branch number and composition in the A/ASBR reactor.

Keywords: A/ASBR, Real-time Quantitative PCR, PAOs Branch, Denitrification

### INTRODUCTION

Eutrophication of water bodies caused by excessive nitrogen and phosphorus discharge is one of the most concerning environmental problems. To reduce its impact, nitrogen and phosphorus in sewage must be removed, especially phosphorus [1,2]. There are chemical and biological methods for phosphorus removal from wastewater, among which the activated sludge method is prominently used [3-8]. The activated sludge system provides suitable environmental conditions to cultivate and domesticate PAOs, which releases phosphorus, synthesizes poly- $\beta$ -hydroxy-alkanoates (PHA), and absorbs phosphorus under aerobic conditions using oxygen as an electron acceptor to transfer phosphorus from sewage to activated sludge. In 1985, Hascote et al. [9] reported that PAOs can absorb phosphorus with  $\text{NO}_3^-$ -N as an electronic receptor, which was the first report on denitrifying phosphorus absorption. The denitrifying phosphorus removal principle is similar to traditional biological phosphorus removal. The phosphorus release process in the anaerobic section is consistent with the traditional process. In the anoxic section, denitrifying phosphorus removal bacteria uses nitrate as the electronic acceptor to absorb phosphorus. In 1987, Comeau and Gerber [10,11] also reported that PAOs were not specific aerobic bacteria, and some PAOs could take  $\text{NO}_3^-$ -N as the electronic receptor. In 1993, Kuba et al. observed through batch-test that PAOs with denitrification function were easily enriched

under the environmental conditions of anaerobic/anoxic alternation. Øtgaard et al. [12] found that about 60% of chemical oxygen demand (COD) was absorbed in the form of PHA in the anaerobic tank in the study on the operation of the actual sewage plant of the University of Cape Town (UCT) process.

In the subsequent anoxic tank, one-third of the COD was consumed in the form of PHA, accompanied by phosphorus absorption. Therefore, the anoxic section in the UCT process played an essential role in enhancing biological phosphorus absorption. As a result, about 30% of phosphate was removed from the anoxic tank. Other research reports pointed out that the improved UCT process strengthened the alternation of an anaerobic/anoxic environment, eliminated other bacteria, and was conducive to the growth of PAOs with denitrifying function [13-15]. Kuba et al. [13] studied the UCT phosphorus removal process in the Holten wastewater treatment plant (WWTP). They found that about 30-50% of the mixed liquid volatile suspended solids (MLVSS) in the efficiently operating plant contained PAOs, and 50% of them had the ability to denitrify.

Numerous studies have reported the existence of denitrification phosphorus absorption, but the performances were quite different, mainly affected by the following factors:  $\text{NO}_3^-$ -N concentration, sludge age, carbon source type and carbon to phosphorus ratio (C/P) and pH value, etc. [16-27]. As an electron acceptor,  $\text{NO}_3^-$ -N greatly influences the denitrification and phosphorus absorption process.

Given the widespread phenomenon of denitrification and phosphorus absorption in the synchronous nitrogen and phosphorus removal system, in 1999, the International Water Association (IWA) expert group introduced the activated sludge reaction kinetic model

<sup>†</sup>To whom correspondence should be addressed.

E-mail: wangxiaoling1977@126.com

Copyright by The Korean Institute of Chemical Engineers.

2d (ASM2d). This was based on activated sludge reaction kinetic model 2 (ASM2), thus adding two processes of PAOs storing phosphorus under anoxic conditions and using PHA to grow [28].

$\frac{S_{NO_3^-}}{K_{NO_3^-} + S_{NO_3^-}}$  is one of the “switching functions” of the denitrification process of common heterotrophic bacteria and the anoxic phosphorus uptake of PAOs, where  $S_{NO_3^-}$  is the  $NO_3^-$ -N concentration in the anoxic section, and  $K_{NO_3^-}$  is the semi-saturated constant (the recommended value of IWA is 0.5 mg/L). This switching function controls the anoxic section's denitrification and phosphorus accumulation storage rate [28]. In addition, Londong [29] showed that to use the denitrification potential fully, the  $NO_3^-$ -N concentration in the anoxic section can be controlled within a non-zero low-value range in the continuous-flow single-sludge synchronous nitrogen and phosphorus removal system. Musvoto et al. [30] showed that in the modified University of Cape Town (MUCT) process, the  $NO_3^-$ -N concentration in the main anoxic section is the main influencing factor in the denitrifying phosphorus absorption process. Wang et al. [31] showed that using the  $NO_3^-$ -N concentration in the main anoxic section as the optimal operation parameter of the continuous-flow single-sludge synchronous nitrogen and phosphorus removal system can reduce the effluent nitrogen and phosphorus concentration. The relationship between the flow and distribution of carbon, nitrogen and phosphorus under different concentrations of  $NO_3^-$ -N was found based on material balance and chemometrics principles.

Furthermore, the reduction effects on carbon source, power consumption and excess sludge production were analyzed and evaluated. Finally, the treatment effect and theoretical principle proved the feasibility of  $NO_3^-$ -N as an operation control parameter. With

the help of engineering technology, the above research results analyzed the relationship between  $NO_3^-$ -N and denitrifying phosphorus absorption from a macro perspective but lacked the support of microbiological principles.

It has been pointed out that PAOs mainly belong to the Rhodochlus Group in Beta proteobacteria and are named *Candidatus Accumilibacter phosphatis* [32]. It is the dominant phosphorus removal microorganism [33,34] that is the most widely used and deeply researched PAOs in urban domestic sewage treatment. Modern molecular biology technology does not rely on pure culture, which is an effective means for qualitative and quantitative analysis of PAOs. For quantitative analysis of PAOs, 16S rRNA is a widely used gene marker quantified by real-time fluorescent quantitative PCR (qPCR) technology. However, 16S rRNA is highly conservative and cannot distinguish the evolutionary branches of *Accumulibacter* [35]. Therefore, using 16S rRNA as a gene marker, molecular biology can only quantify the abundance of all PAOs and cannot quantify different evolutionary branches. Macrogenomic analysis shows that *Accumulibacter* has a single copy of the *ppk1* encoding gene [36], which plays an essential role in the polyphosphate (poly-P) transformation in *Accumulibacter*. Therefore, the *ppk1* functional gene has become a gene marker for studying the evolutionary branch of *Accumulibacter*.

There are many evolutionary branches of *Accumulibacter*, and the utilization ability of  $NO_3^-$ -N of each evolutionary branch is significantly different [37,38]. This paper uses the A/ASBR to measure the phosphorus accumulating microbial population with the configured sewage as the treatment object. The fluorescence real-time quantitative PCR technology is used to study the relationship between the number and composition of the activated sludge microbial population, the number and composition of *Accumulibacter* IA, IIA, IIB, IIC, IID, and IIF, and the change of  $NO_3^-$ -N concen-

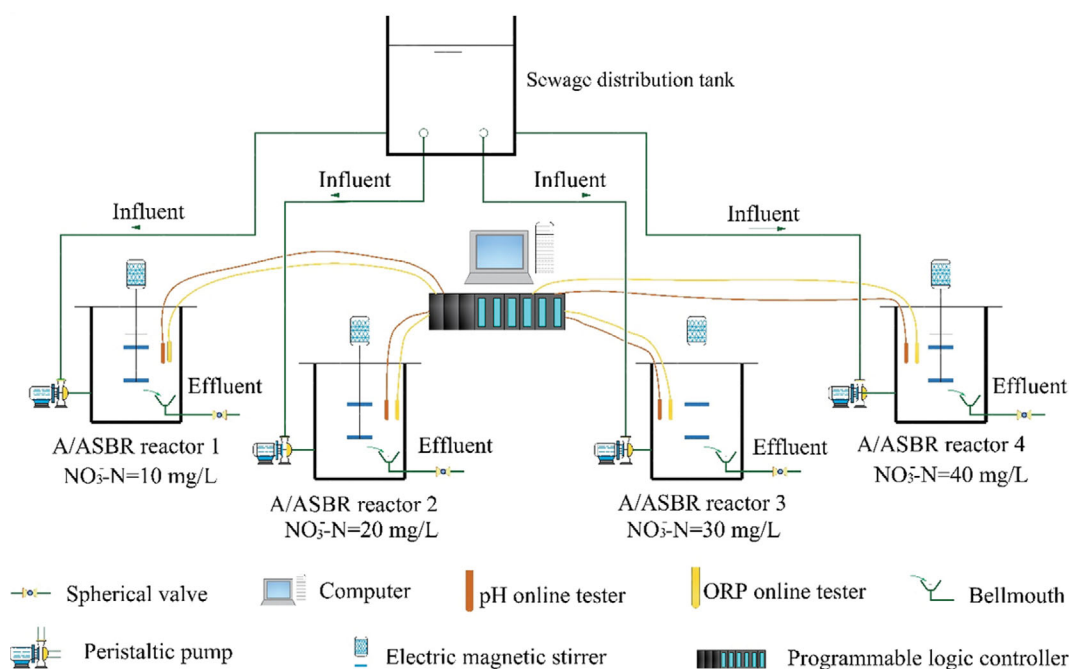


Fig. 1. Test device.

**Table 1. Composition and water quality characteristics of simulated wastewater**

Compound composition	Dosage	Trace element composition	Concentration g/L
Acetic acid	3 mL	FeCl <sub>3</sub>	0.9
KH <sub>2</sub> PO <sub>4</sub>	0.6 g/L	H <sub>3</sub> BO <sub>4</sub>	0.15
NaHCO <sub>3</sub>	5 g/L	CoCl <sub>2</sub> ·7H <sub>2</sub> O	0.15
CaCl <sub>2</sub>	0.2 g/L	CuSO <sub>4</sub> ·5H <sub>2</sub> O	0.03
MgSO <sub>4</sub>	1.0 g/L	KI	0.18
Trace element solution	12 L	MnCl <sub>2</sub> ·4H <sub>2</sub> O	0.06
		Na <sub>2</sub> Mo·2H <sub>2</sub> O	0.06
		ZnSO <sub>4</sub> ·7H <sub>2</sub> O	0.12

tration, to determine the microbial population structure and its driving factors, and to combine the microbiological community with the macro function of the system. Furthermore, to achieve the purpose of effectively regulating the stability of the system and optimizing its functions.

## MATERIALS AND METHODS

### 1. Test Device

The test device and process are shown in Fig. 1. A batch test was carried out in four A/ASBR reactors with an effective volume of 4.5 L. The reactor diameter was 15 cm, the height was 35 cm, and the superlevation was 10 cm. A drainage bell was set 5 cm away from the bottom of the reactor. The WTW inolab pH probe and oxidation-reduction potential (ORP) probe were set in the A/ASBR device, and the stirrers were set in the reactors to ensure the uniform mixing of sludge and water. To prevent the aerobic phosphorus absorption process, the top of the reactor was covered. A sewage distribution tank channelled water as influent into the A/ASBR reactor. The effective volume of the sewage distribution tank was 16.4 L (thus, L×B×H=20 cm×20 cm×50 cm), of which the superlevation was 9 cm. One water outlet was set at the middle position 5 cm away from the bottom of the four sides of the tank, which was connected with the peristaltic pumps of the four reactors (A/ASBR reactor 1, A/ASBR reactor 2, A/ASBR reactor 3 and A/ASBR reactor 4) for inlet water, respectively. The four A/ASBR reactors were independent.

During the test, the sewage in the water distribution tank entered the reactors through the peristaltic pumps. The treated water was discharged from the system through the outlet bell mouths after the biochemical reactions and precipitation processes were completed. In the reaction processes, the values of pH and ORP were measured in real-time and transmitted to the PLC (programmable logic controller) system in the computer to monitor and control the operating environments.

### 2. Experiment Scheme

Synthetic sewage was used in the experiment; acetic acid was added as a carbon source, and KH<sub>2</sub>PO<sub>4</sub> was added as a source of phosphorus salt in the influent. NaHCO<sub>3</sub> was added to maintain the pH value in the neutral range during the reaction, and MgSO<sub>4</sub> and CaCl<sub>2</sub> were added to meet the requirements of Mg<sup>2+</sup> and Ca<sup>2+</sup> ions in the process of phosphorus uptake by PAOs. In addition, trace element solutions were added to meet the nutritional require-

ments of the growth and reproduction of activated sludge microorganisms. See Table 1 for the dosage and water quality characteristics of each component of simulated wastewater.

The inoculated sludge introduced in the A/ASBR reactor was transferred from the aerobic section of the MUCT reactor with an effective volume of 90 L operated in the laboratory. The system has been running for nearly two years, treating domestic sewage with COD/total nitrogen (TN) lower than 6. When extracting the inoculated sludge, the operating parameters of the reactor were as follows: the treated water volume was 10 L/h, the sludge load was (0.253±0.071) kg/(kg·d), the sludge reflux ratio was 0.5, the mixed liquid reflux ratio was 1.0, the sludge age was 12 days, and the NO<sub>3</sub><sup>-</sup>-N concentration in the main anoxic section was 2.5 mg/L. At this time, the system's denitrification and phosphorus removal effect were good, and the phenomenon of phosphorus absorption in the anoxic zone was evident. Furthermore, the material balance calculation results showed that the anoxic phosphorus absorption rate of the system (the percentage of anoxic phosphorus absorption in the total phosphorus absorption) was stable at about 47% [31].

After the sludge was taken out, it was inoculated into the four A/ASBR reactors, and the initial mixed liquor suspended solids (MLSS) concentration was 1,500 mg/L. The reactor was operated in cycles, 8 h per cycle, including water inflow 5 min, anaerobic 2 h, anoxic 4 h, sedimentation 1.5 h, and drainage/sludge 25 min; thus, one cycle per day. The water inflow of each reactor was 3.6 L per cycle. To ensure that the inlet water quality was identical, the wastewater to be treated was configured in one sewage distribution tank. After mixing evenly, the wastewater was pumped into their respective A/ASBR reactor using a longer peristaltic pump (driver bt600-2j, pump head yz2515x, flow range 0.07 mL/min-3,000 mL/min, Baoding, China), one for each reactor. The hydraulic method was adopted to control the sludge age to 15 d [39]. To prevent phosphate precipitation caused by increased pH value in the phosphorus absorption process (phosphate precipitation could occur when the pH value was more significant than 8.5). The reaction process was monitored online with a pH meter, and the pH value of the reaction process system was maintained within the range of 7.0±0.1 by adding dilute HCl or NaOH solution.

After the anaerobic phosphorus release reaction, different amounts of potassium nitrate (0.30, 0.60, 0.90, 1.20 g) were added to the reactor to enter the anoxic phosphorus absorption section. The four A/ASBRs were named A/ASBR1, A/ASBR2, A/ASBR3, and A/

ASBR4 according to the different dosages of potassium nitrate. The reactors were operated for 30 cycles, the effects of phosphorus release, phosphorus absorption, and denitrification remained stable, and samples were taken for experimental research.

### 3. Conventional Water Quality Indexes and Testing Methods

Water samples were taken from the drainage bell set at 5 cm from the bottom of the A/ASBR reactor during the test. After the influent volume in the reactor reached its target, sampling in the anaerobic section started and the reaction time was recorded as 0 min. Samples were taken at intervals of 15 min within 0-60 min; 30 min intervals within 60-120 min; sampling at 15-min interval within 120-180 min; sampling at 30-min interval with 180-240 min; sampling at 60-min interval within 240-360 min. Among them, the water sample at 0 min was the influent water sample and the water sample at 360 min was the effluent water sample. The water samples were centrifuged at 4,500 rpm for 7 min, and the supernatant was collected. The indexes of COD, total phosphorus (TP),  $\text{NH}_4^+$ -N,  $\text{NO}_3^-$ -N, and  $\text{NO}_2^-$ -N were determined by the standard method [40].

### 4. Deoxyribonucleic Acid (DNA) Extraction and Purification

At the end of the experiment, a certain amount of evenly mixed

mud water mixture was extracted from the four A/ASBR reactors. After high-speed freezing and centrifugation to remove excess water, it was freeze-dried at  $-80^\circ\text{C}$  and stored for inspection. About 0.1 g of sample was weighed and DNA was extracted using MP Soil DNA Rapid Extraction Kit (Bio 101, Vista, CA, USA) regarding the instructions for the kit for specific methods. DNA concentration was determined using a nanodrop spectrophotometer ND-1000 (Thermo Fisher Scientific, USA) microspectrophotometer. The subsequent analysis stage was entered when the extraction quality met the requirements.

### 5. Real-time Quantitative PCR Test

The fluorescent real-time quantitative reaction was performed on the Mx3005P real-time quantitative PCR amplification instrument (Agilent Technologies, USA), using a 25  $\mu\text{L}$  reaction system (Brilliant II SYBR Green qPCR (real-time fluorescent quantitative PCR) Master Mix, Agilent Technologies, USA). The reaction system is shown in Table 2 [37]. Bacterial 16S rRNA gene, total *Candidatus accumulibacter* 16S rRNA gene and *Candidatus accumulibacter* specific functional gene *ppk* were used to quantify the absolute abundance of whole bacteria, total *Accumulibacter* and *Accumulibacter* IA, *Accumulibacter* IIA, *Accumulibacter* IIB, *Accumulibacter*

**Table 2. qPCR reaction mixture**

Reaction component	Volume	Final concentration
Brilliant II SYBR Green qPCR master mix (2x)	12.5 $\mu\text{L}$	1X
Forward primer 10 mM	1 $\mu\text{L}$	400 nM
Reverse primer 10 mM	1 $\mu\text{L}$	400 nM
ROX	0.5 $\mu\text{L}$	40 nM
Sterile water	8 $\mu\text{L}$	-----
DNA template	2 $\mu\text{L}$	-----

**Table 3. Specific primer sequences and programs of qPCR**

Primer	Sequence	Amplification size (bp)	Target	Program
1055f	ATGGCTGTCGTCAGCT	323	Bacterial 16S rRNA	95 $^\circ\text{C}$ 10 min; (95 $^\circ\text{C}$ 30 s, 50 $^\circ\text{C}$ 60 s, 72 $^\circ\text{C}$ 20 s) $\times$ 45
1392r	ACGGGCGGTGTGTAC			
518f	CCAGCAGCCGCGGTAAT	351	Acc 16S rRNA	95 $^\circ\text{C}$ 3 min; (94 $^\circ\text{C}$ 30 s, 60 $^\circ\text{C}$ 45 s, 72 $^\circ\text{C}$ 30 s) $\times$ 35
PAO-846r	GTTAGCTACGGCACTAAAAGG			
Acc-ppk1-763f	GACGAAGAAGCGGTCAAG	408	Acc-IA	95 $^\circ\text{C}$ 3 min; (94 $^\circ\text{C}$ 30 s, 63 $^\circ\text{C}$ 45 s, 72 $^\circ\text{C}$ 30 s) $\times$ 45
Acc-ppk1-1170r	AACGGTCATCTTGATGGC			
Acc-ppk1-893f	AGTTCAATCTCACCGAGAGC	105	Acc-IIA	95 $^\circ\text{C}$ 3 min; (94 $^\circ\text{C}$ , 30 s, 61 $^\circ\text{C}$ 45 s, 72 $^\circ\text{C}$ 30 s) $\times$ 45
Acc-ppk1-997r	GGAACCTCAGGTCGTTGC			
Acc-ppk1-870f	GATGACCCAGTTCCTGCTCG	133	Acc-IIB	95 $^\circ\text{C}$ 3 min; (94 $^\circ\text{C}$ 30 s, 61 $^\circ\text{C}$ 45 s, 72 $^\circ\text{C}$ 30 s) $\times$ 45
Acc-ppk1-1002r	CGGCACGAACCTCAGATCG			
Acc-ppk1-254f	TCACCACCGACGGCAAGAC	207	Acc-IIC	95 $^\circ\text{C}$ 3 min; (94 $^\circ\text{C}$ 30 s, 66 $^\circ\text{C}$ 45 s, 72 $^\circ\text{C}$ 30 s) $\times$ 45
Acc-ppk1-46Or	CCGGCATGACTTCGCGGAAG			
Acc-ppk1-1123f	GAACAGTCCGCCAACGACC	254	Acc-IIC (ppk1 excluding OTU NSD3)	95 $^\circ\text{C}$ 3 min; (94 $^\circ\text{C}$ 30 s, 63 $^\circ\text{C}$ 45 s, 72 $^\circ\text{C}$ 30 s) $\times$ 45
Acc-ppk1-1376r	ACGATCATCAGCATCTTGGC			
Acc-ppk1-375f	GGGTATCCGTTTCTCAAGCG	148	Acc-IID	95 $^\circ\text{C}$ 3 min; (94 $^\circ\text{C}$ 30 s, 63 $^\circ\text{C}$ 45 s, 72 $^\circ\text{C}$ 30 s) $\times$ 45
Acc-ppk1-522r	GAGGCTCTTGTGAGTACACGC			
Acc-ppk1-355f	CGAACTCGGCGAAAGCGAGTA	246	Acc-IIF	95 $^\circ\text{C}$ 3 min; (94 $^\circ\text{C}$ 30 s, 70 $^\circ\text{C}$ 45 s, 72 $^\circ\text{C}$ 30 s) $\times$ 45
Acc-ppk1-600r	ATCGCTCCGAGCAACTGTTC			

IIC, Accumulibacter IID and Accumulibacter IIE, respectively. See Table 3 for primer sequence, reaction system and temperature rise procedure. To ensure the validity of the data results, the standard curve was established by ten times gradient dilution of plasmid DNA with known concentration. The standard and tested samples were set three parallel and the negative control was set. The linear values of the fluorescence quantitative standard curve all satisfied  $R^2 > 0.98$  and the amplification efficiency was 80%-120%. The single peak curve was specific amplification. According to the known copy number of the standard sample, the quantitative standard curve was obtained through the fluorescence threshold and cycle number Ct value of the standard sample in the quantitative process. Then the copy number of the DNA sample to be tested was calculated according to the Ct value of the sample to be tested given by the system [37,41,42].

## RESULTS AND DISCUSSION

### 1. Analysis of Phosphorus Removal Performance of A/ASBR

After the successful start-up of the reactor, samples were taken for analysis. During stable operation, the water quality indicators such as COD, TP and  $\text{NO}_3^-$ -N of the influent and removal rates of the reactor effluent are shown in Table 4.

According to the principle of denitrifying phosphorus absorption, the phosphorus removal efficiency of the A/ASBR reactor was mainly affected by  $\text{NO}_3^-$ -N. According to the principle of simultaneous nitrogen and phosphorus removal and denitrifying phosphorus absorption. The  $\text{NO}_3^-$ -N added in the A/ASBR reactor was mainly removed through the common denitrification process with COD as the carbon source and the denitrifying phosphorus absorption process with poly- $\beta$ -hydroxy-butyrate (PHB) stored in the PAOs as the carbon source. According to the research report, the reaction rate of the ordinary denitrification process was significantly higher than that of the denitrification phosphorus absorption process; that is, when there is COD in the reactor, the ordinary denitrification process will be carried out preferentially [43]. It can

be seen from Table 4 that with the increase of  $\text{NO}_3^-$ -N dosage in the four A/ASBR reactors, the ratio of influent COD and  $\text{NO}_3^-$ -N in the anoxic section decreased from 17.42 to 4.44. Denitrifying bacteria are heterotrophic bacteria, so no matter which method is used to remove  $\text{NO}_3^-$ -N, its removal rate is related to the COD/ $\text{NO}_3^-$ -N ratio; that is, with the reduction of this ratio, the removal rate of  $\text{NO}_3^-$ -N decreases. When the ratio dropped to 4.44, the denitrification carbon source was insufficient, so the concentration of  $\text{NO}_3^-$ -N effluent increased and the removal rate decreased.

In the A/ASBR system,  $\text{NO}_3^-$ -N was the only electron acceptor in the phosphorus absorption process. Therefore, the larger the dosage, the more sufficient electron acceptors were provided, and the more suitable it was for cultivating and domesticating denitrifying phosphorus accumulating bacteria. Therefore, in A/ASBR1 and A/ASBR2, the dosing concentration of  $\text{NO}_3^-$ -N was low and the electron acceptor of denitrifying phosphorus uptake was limited, resulting in the reduction of glycogen storage during phosphorus uptake, affecting the PHB synthesis during phosphorus release. Consequently, the phosphorus removal effect was poor. TP removal rates were only 48.86% and 66.34%. However, when the  $\text{NO}_3^-$ -N concentration in the anoxic section was increased to 30 mg/L and 40 mg/L, the electron acceptor was sufficient and the total phosphorus removal effect was excellent, increasing to 86.62% and 92.00%, respectively.

The four A/ASBR reactors were operated for about 80 cycles. See Fig. 2 for the variation of TP, COD and  $\text{NO}_3^-$ -N concentration with reaction time in the 75 th typical operation cycle. It can be seen that the degradation of COD in the four reactors presented the following variation law: it stopped/slowed after early rapid consumption and then increased the removal rate after the addition of  $\text{NO}_3^-$ -N. The activated sludge degraded pollutants mainly in the early stage of the biosorption process at a fast rate, so the COD concentration in the sewage in the early stage decreased rapidly. Then, the adsorbed COD was absorbed and transformed by phosphorus accumulating bacteria and denitrifying bacteria as a nutrient, showing a slight decrease in COD concentration. In the

**Table 4. Quality characteristics of influent and effluent water during stable operation**

Reactor	Indicator (mg/L)	Influent (mg/L)	Effluent (mg/L)	Removal rate (%)	Influent COD/ $\text{NO}_3^-$ -N
A/ASBR1	COD	175.06±5.56	38.09±4.78	78.24±4.21	17.42±1.98
	TP	8.31±0.98	4.25±1.01	48.86±0.88	
	$\text{NO}_3^-$ -N	10.05±0.97	0.98±0.45	90.25±0.75	
A/ASBR2	COD	167.31±6.01	34.56±4.21	79.34±5.05	8.23±1.54
	TP	8.17±1.12	2.75±0.86	66.34±1.04	
	$\text{NO}_3^-$ -N	20.32±1.04	2.86±0.98	85.93±1.03	
A/ASBR3	COD	182.43±5.32	36.54±4.97	79.97±4.53	6.35±2.17
	TP	7.85±1.23	1.12±0.43	86.62±0.87	
	$\text{NO}_3^-$ -N	28.72±0.95	4.97±0.76	82.69±0.91	
A/ASBR4	COD	175.43±6.12	35.75±4.59	76.62±5.87	4.44±1.97
	TP	8.37±1.09	0.67±0.76	92.00±1.04	
	$\text{NO}_3^-$ -N	39.47±1.16	11.54±1.07	70.76±1.15	

Note: The concentration data of each indicator in the table is mean value±standard deviation (n=60, p=0.683).

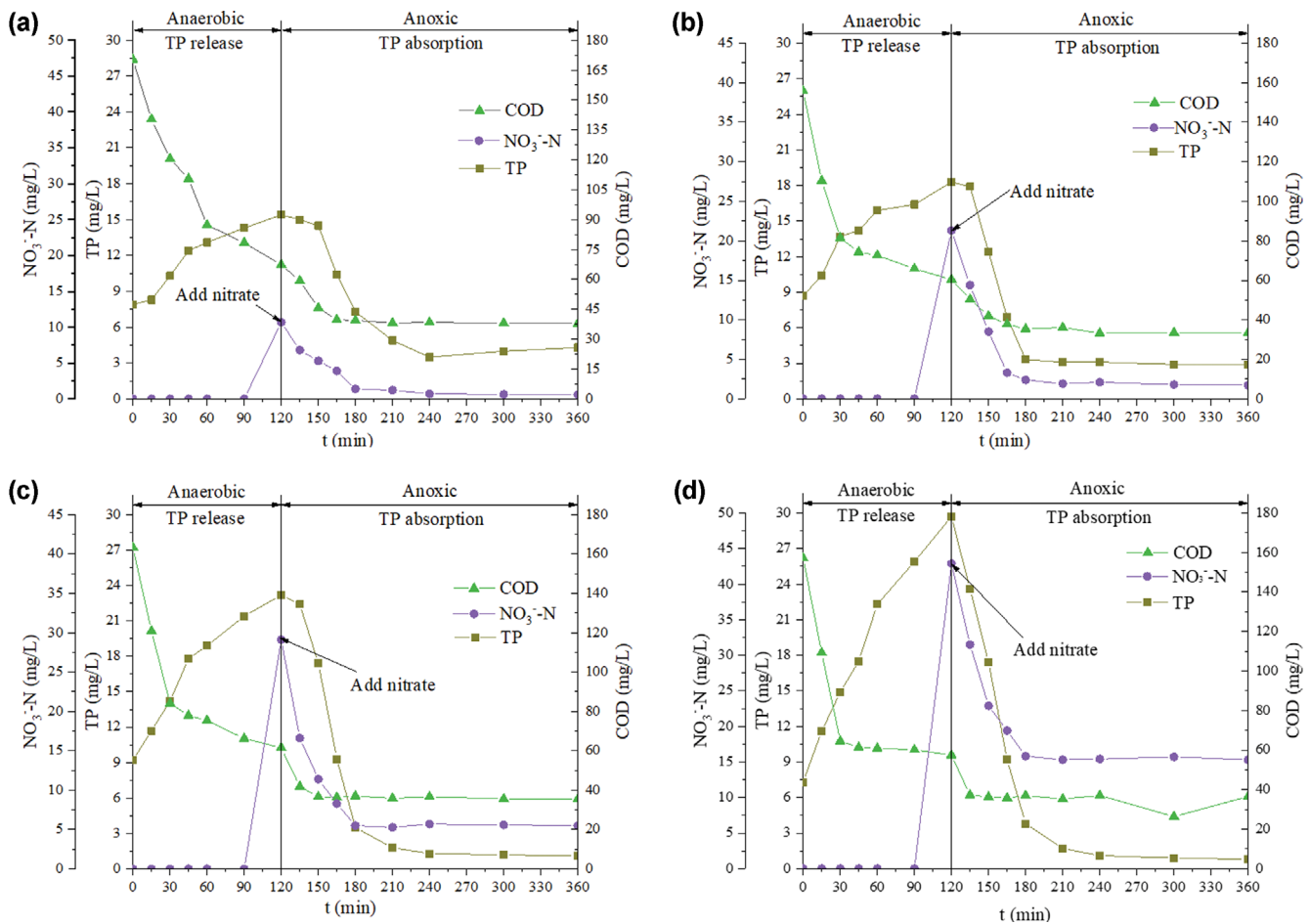


Fig. 2. The typical variation law of each index with the variation of  $\text{NO}_3^-$ -N dosage. (a)  $\text{NO}_3^-$ -N=10 mg/L; (b)  $\text{NO}_3^-$ -N=20 mg/L; (c)  $\text{NO}_3^-$ -N=30 mg/L; (d)  $\text{NO}_3^-$ -N=40 mg/L.

anoxic section, because  $\text{NO}_3^-$ -N was used as an electron acceptor, the denitrification rate was more significant than the rate of COD conversion to PHA and the anaerobic digestion rate, so the COD degradation rate in sewage increased at this time.

Phosphorus absorption and nitrate reduction in the four reactors were carried out simultaneously (Fig. 2), indicating that denitrifying phosphorus absorption reaction had taken place, which proved that there were PAOs with denitrifying function in the activated sludge. However, the phosphorus release and absorption of the four reactors were different and increased with the increase of  $\text{NO}_3^-$ -N concentration; the phosphorus release was 7.52, 9.61, 15.00 and 22.31 mg/L, respectively, and the phosphorus absorption was 11.17, 15.40, 22.01 and 28.97 mg/L, respectively. Furthermore, from Fig. 2(a), when the  $\text{NO}_3^-$ -N dosing concentration was 10 mg/L, the  $\text{NO}_3^-$ -N concentration in the reactor was very low after 210 min of the reaction, resulting in an anaerobic state and endogenous respiratory phosphorus release reaction, i.e., invalid phosphorus release, resulting in a slight increase in the TP concentration of subsequent effluent. On the other hand, when the  $\text{NO}_3^-$ -N concentration was increased to 20 mg/L, 30 mg/L and 40 mg/L, respectively, the electron acceptor was sufficient, the reactor was always anoxic state, and no invalid phosphorus release occurred.

It can also be seen from Fig. 2 that the phosphorus release rate

and  $\text{NO}_3^-$ -N reaction rate of each reactor at the initial stage of anaerobic and anoxic were high, and then with the extension of reaction time at each stage the reaction rates of phosphorus release and  $\text{NO}_3^-$ -N gradually slowed. In addition, the initial phosphorus release rate increased with the increase of nitrate concentration. In the anoxic section, the denitrifying phosphorus uptake rate changed considerably under different  $\text{NO}_3^-$ -N concentrations, increasing from 2.00 mg/(L·h) of 10 mg/L  $\text{NO}_3^-$ -N to 24.42 mg/(L·h) of 40 mg/L  $\text{NO}_3^-$ -N. The reason may be that the dosing concentration of  $\text{NO}_3^-$ -N in A/ASBR1 was low for a long time, the abundance of phosphorus accumulating bacteria in activated sludge was low, the quantity of COD converted into PHA in influent was small, and part of nitrate in sewage was degraded with COD as carbon source. Therefore, the denitrifying phosphorus absorption rate was low or even at zero in the early stage of anoxia. However, the  $\text{NO}_3^-$ -N concentration in A/ASBR3 and A/ASBR4 was relatively high, because the reactors constantly alternated in the anaerobic/anoxic environment. Many phosphorus-accumulating bacteria with denitrifying functions were cultivated and domesticated. As a result, the quantity of COD in the influent that was converted into PHA increased. Most of the  $\text{NO}_3^-$ -N added was denitrified with PHA as the carbon source. Therefore, the phosphorus absorption rate was high in the early stage of anoxia.

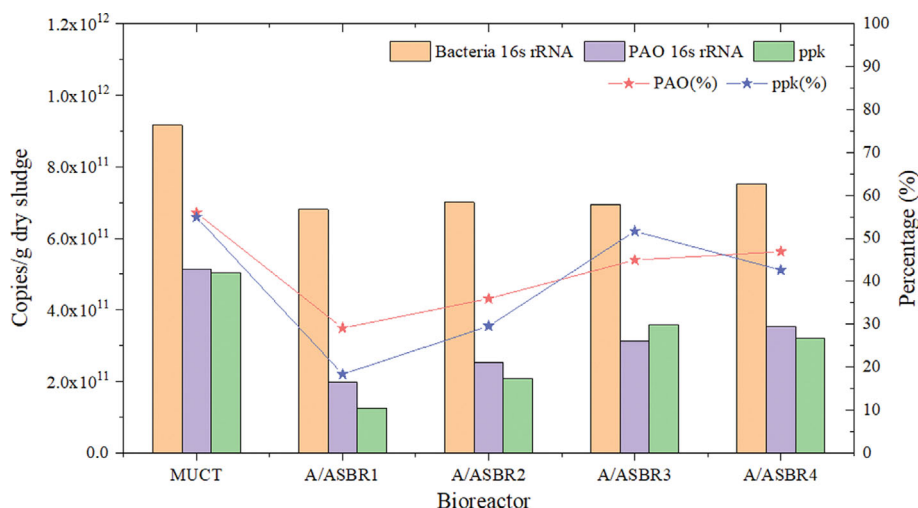


Fig. 3. The number and percentage of 16S rRNA and ppk genes of A/ASBR PAOs.

## 2. The variation of absolute abundance of PAOs in the A/ASBR system driven by $\text{NO}_3^-$ -N

During the test, the real-time quantitative PCR determination of bacteria inoculated with sludge and activated sludge of A/ASBR reactor, 16S rRNA of PAOs and ppk gene of PAOs is shown in Fig. 3. In the figure, the ppk gene was the sum of ppk genes of all branches of PAOs. PAOs (%) and ppk (%) refer to the percentage of 16S rRNA of PAOs and the sum of ppk genes in 16S rRNA of bacteria.

The real-time quantitative PCR detection showed that the gene numbers of inoculated sludge bacteria 16S rRNA, PAOs 16S rRNA and ppk were  $9.17 \times 10^{11}$  copies/g dry sludge,  $5.13 \times 10^{11}$  copies/g dry sludge and  $5.04 \times 10^{11}$  copies/g dry sludge, respectively. The percentages of PAOs 16S rRNA and ppk genes were 55.94% and 54.95%, respectively, with a slight difference. Previous research calculated the cell material production of PAOs and the total bacteria by taking the MUCT reactor as the system boundary, based on the principles of material balance and stoichiometry and according to carbon distribution and flow law, nitrogen, and phosphorus. Among them, the production of PAOs accounted for 57.15% of the total bacteria, similar to the result of gene quantity determination of PAOs. In Fig. 3 the number of 16S rRNA genes in the four A/ASBR reactors was basically the same, between  $6.81 \times 10^{11}$ – $7.53 \times 10^{11}$  copies/g dry sludge, but they were all lower than that of the inoculated sludge. On the other hand, with the increase in  $\text{NO}_3^-$ -N concentration, PAOs amount (absolute abundance) in the A/ASBR reactor increased, and the proportion gradually increased. For example, when the  $\text{NO}_3^-$ -N concentration was 10 mg/L, the quantity of PAOs 16S rRNA and ppk genes was  $1.98 \times 10^{11}$  copies/g dry sludge and  $1.25 \times 10^{11}$  copies/g dry sludge, respectively, and the percentage was 29.07% and 18.32%, respectively. However, when the  $\text{NO}_3^-$ -N dosage was 30 mg/L, they were  $3.12 \times 10^{11}$  copies/g dry sludge and  $3.59 \times 10^{11}$  copies/g dry sludge, and the percentages were 44.95% and 51.07%, respectively.

It can also be seen from Fig. 3 that when the  $\text{NO}_3^-$ -N dosage was about 40 mg/L, the number of Acc 16S rRNA genes of phosphorus accumulating bacteria increased to  $3.53 \times 10^{11}$  copies/g dry

sludge, but the increase rate decreased. As a result, the number of ppk genes decreased to  $3.21 \times 10^{11}$  copies/g dry sludge. The increase in the number of Acc 16S rRNA genes of phosphorus accumulating bacteria was due to the increased concentration of  $\text{NO}_3^-$ -N, which provided more electron receptors and promoted the growth and reproduction of more PAOs. However, the decrease in the ppk gene can be attributed to more unmeasured PAO branches being cultivated and grown with the increase of  $\text{NO}_3^-$ -N concentration in the system. Mao et al. [43] reported that, besides the seven branches detected in this paper, there are also Accumulibacter IB, IC, ID, IE, IIE, IIG, IIHand other branches. He et al. [35] also reported that phosphorus accumulating bacteria could be divided into 12 branches. Therefore, it can be inferred that  $\text{NO}_3^-$ -N and its dosage were the main driving factors for changing PAOs quantity and composition in the A/ASBR reactor.

## 3. Variation in the Number and Composition of Each Branch of PAOs Driven by $\text{NO}_3^-$ -N

According to the real-time quantitative PCR results of the ppk gene in each branch of PAOs, all seven branches were present in each activated sludge sample, indicating that the MUCT system and A/ASBR system maintained a high diversity of branches. The detection results are shown in Fig. 4. The percentage in the figures was the percentage of each branch content in the total ppk gene. It can be seen from Fig. 4(a) that Accumulibacter IIC is dominant in all reactors under different  $\text{NO}_3^-$ -N concentrations and its content is much higher than that of other branches. When the  $\text{NO}_3^-$ -N concentration is 30 mg/L, the quantity of Accumulibacter IIC and IIC(ppk) is the highest. In addition, IIC and IIC (ppk1 excluding OTU NS D3), as two subspecies of the IIC branch, have different abundance changes in the whole system. IIC, compared with IIC (ppk1 excluding OTU NS D3), has an apparent competitive advantage, and its quantity increases with the increase of  $\text{NO}_3^-$ -N concentration, thus accounting for 84.53% of the total Accumulibacter. The number of IA and IID branches also increased with the  $\text{NO}_3^-$ -N concentration, but the percentage of the two branches changed little, close to that of the inoculated sludge.

Previous studies pointed out that when the actual domestic sew-

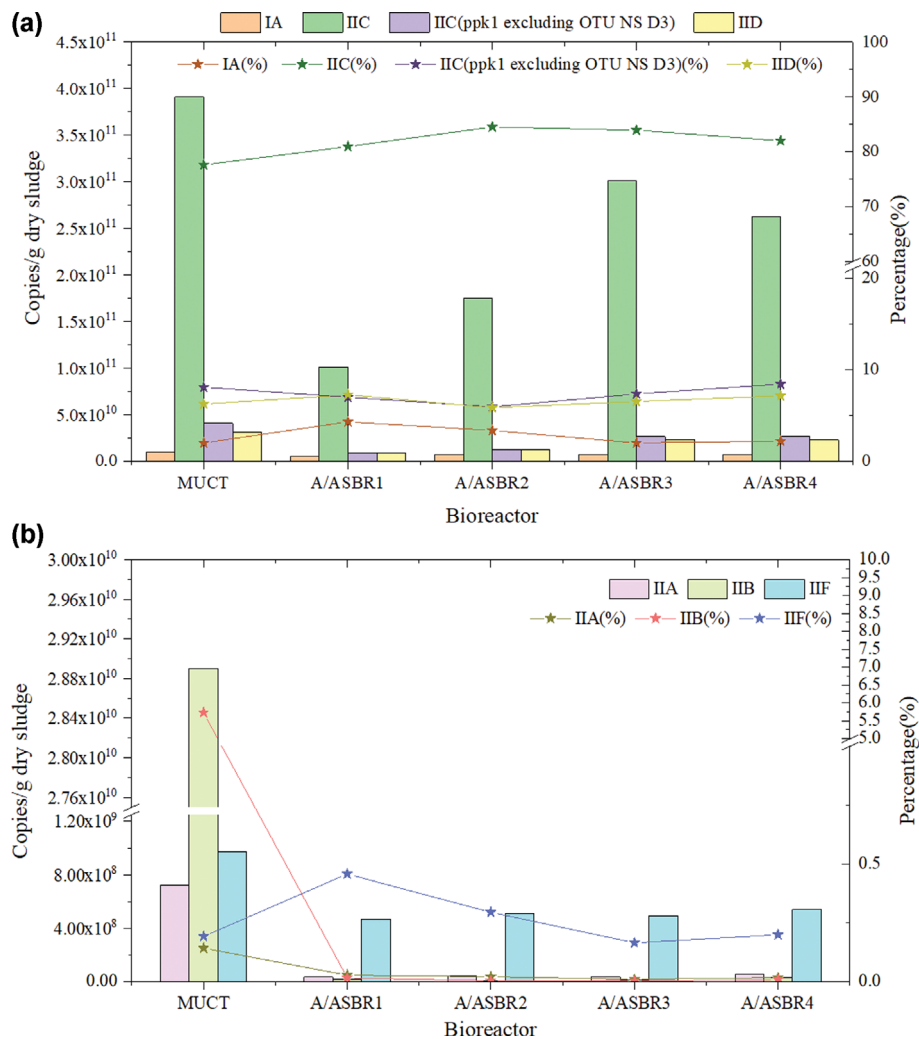


**Fig. 4. Absolute abundance and content of PAOs branches. (a) Absolute abundance and content of Accumulibacter IA, IIC and IID; (b) Absolute abundance and content of Accumulibacter IIA, IIB and IIF.**

age was treated in the continuous flow process, the Accumulibacter IIC and IID branches had strong denitrifying phosphorus removal capacity, which is similar to the results of this study [44,45]. Another research report pointed out that in the pilot sequencing batch reactor (SBR), the enriched Accumulibacter IIC showed strong  $\text{NO}_3^-$ -N removal capacity. Nevertheless, the literature also points out that not all denitrification contributions can be attributed to this branch [46]. According to the genome sketch results of Accumulibacter IIC, the bacterium lacked nitric oxide reductase (nor) and nitrous oxide reductase (nos) genes and did not have a complete denitrification metabolic pathway. Therefore, it was speculated that other flanking denitrifying bacteria might be involved in denitrifying phosphorus uptake [47]. This may also be why the ppk gene copy number of Accumulibacter IIC decreased when the  $\text{NO}_3^-$ -N dosage increased to 40 mg/L. Therefore, the synergistic mechanism of denitrifying functional flora needed to be further studied. When Accumulibacter IID existed in activated sludge and its content was high,  $\text{NO}_3^-$ -N,  $\text{NO}_2^-$ -N and oxygen could be used as electron receptors to achieve good nitrogen and phosphorus removal effect [27], which is consistent with the results of this study. This was the rea-

son for the high absolute abundance of IID branches in activated sludge.

It has been proved that the Accumulibacter IA branch can use  $\text{NO}_3^-$ -N for denitrifying phosphorus absorption, and it can be seen from the above Fig. 4(a) that the number of this branch gradually increased with the increase of  $\text{NO}_3^-$ -N concentration from  $5.37 \times 10^9$  copies/g dry sludge increased to  $7.17 \times 10^9$  copies/g dry sludge. Furthermore, Chao et al. showed that when  $\text{NO}_3^-$ -N was the electron acceptor, the proportion of PAOs in the whole bacteria in the SBR reactor decreased from the initial 2.8% to 0.6%. However, the phosphorus removal performance of the system was enhanced, which may be because Accumulibacter IA with  $\text{NO}_3^-$ -N as the electron acceptor was enriched. Hence, consistent with the research result, IA accounted for a relatively high proportion [48].

Therefore, with the increase of  $\text{NO}_3^-$ -N dosing concentration, the number of copies of Accumulator IA and Accumulator IID genes increased, respectively. In contrast, the number of Accumulator IIC and Accumulator IIC (ppk1 excluding OTU NS D3) showed an overall increasing trend (decreased at 40 mg/L). This indicates that  $\text{NO}_3^-$ -N gradually provided sufficient electron recep-

tors for A/ASBR, promoted the alternative circulation of activated sludge in an anaerobic/anoxic environment, and domesticated more PAOs branches with denitrifying functions. This was consistent with the above experimental conclusion that the higher the  $\text{NO}_3^-$ -N concentration, the lower the total phosphorus concentration in the effluent, and the better the phosphorus removal effect. Therefore, the change in the number and composition of PAOs was the microbiological explanation for the effect of denitrifying phosphorus removal.

It can be seen from Fig. 4(b) that the absolute abundance of branches IIA, IIB and IIF was statistically significantly lower than that of other branches, indicating that they contributed less to the whole process (not the core genus). Metagenomic analysis showed that the IIA branch could not utilize  $\text{NO}_3^-$ -N because it did not have nitrate reductase (*nar*) [48]. Flowers [49] designed a 16S rRNA fluorescence in situ hybridization (FISH) probe to analyze two different types of branches of *Candidatus Accumulibacter*. It was considered that the IA branch hybridized with probe Acc-I-444 had  $\text{NO}_3^-$ -N removal ability and the corresponding cell shape was rod type. However, the IIA branch hybridized with probe Acc-II-444 did not have nitrogen removal ability and was spherical. This result is consistent with the previous metagenomic results and Carvalho et al. [50].

It can also be seen from Fig. 4(b) that the number of IIB branches in the inoculated sludge was  $2.89 \times 10^{10}$  copies/g dry sludge and a percentage of 5.74% of the total *ppk* gene of PAOs. However, the proportion gradually decreased during the later culture. The quantity of the four A/ASBRs was  $2.08 \times 10^7$  copies/g dry sludge,  $9.65 \times 10^6$  copies/g dry sludge,  $1.07 \times 10^7$  copies/g dry sludge,  $3.12 \times 10^7$  copies/g dry sludge, respectively. The proportion was very low, close to zero. This may be due to the physiological and biochemical characteristics of the strain itself. Some studies have suggested that branch IIB can use  $\text{NO}_3^-$ -N as an electron acceptor, which may be the reason why the branch had not been wholly elutriated out of the system. Branch IIF contained the periplasmic nitrate reductase gene (*nap*), which can use  $\text{NO}_3^-$ -N as an electron acceptor. However, it only accounted for a small proportion of PAOs in the inoculated sludge and A/ASBR system and had never become a dominant bacterium.

To sum up, the inoculated sludge of the four A/ASBR reactors in this study was from the same reactor simultaneously, and the treated wastewater was from the same distribution tank. Except that the  $\text{NO}_3^-$ -N concentration was different at the end of anaerobic and the initial stage of anoxia, other operating parameters and cycles were precisely the same. Therefore, it can be inferred that the main driving factor for the change in the quantity and composition of activated sludge microbial PAOs and each branch was the concentration of  $\text{NO}_3^-$ -N.

In this study, the response law of the number and composition of phosphorus accumulating bacteria and their branches to the change of  $\text{NO}_3^-$ -N dosing concentration was consistent with the macro research results of the impact of  $\text{NO}_3^-$ -N on denitrifying phosphorus absorption performance in the earlier stage [14-16,31]. The combination of the two can provide a scientific basis for developing macro-control parameters and strategies for the simultaneous nitrogen and phosphorus removal system and achieving the

stability of the effective control system and the purpose of functional optimization.

## CONCLUSIONS

This study determined whether the concentration of  $\text{NO}_3^-$ -N is the driving factor of PAOs bacterial population structure under anoxic conditions. The A/ASBR reactor was operated to conduct a fluorescence real-time quantitative PCR test. In addition, the composition and structure changes of phosphorus accumulating bacteria and their branches under different  $\text{NO}_3^-$ -N concentrations were investigated. The test conclusions are as follows:

1. The absolute abundance of the 16S rRNA gene in the A/ASBR reactor had nothing to do with the  $\text{NO}_3^-$ -N, which was at  $6.81 \times 10^{11}$  -  $7.53 \times 10^{11}$  copies/g dry sludge.
2. With the increase of  $\text{NO}_3^-$ -N concentration, the amount (absolute abundance) of PAOs in the A/ASBR reactor increased, and the proportion gradually increased. The  $\text{NO}_3^-$ -N dosage increased from  $1.98 \times 10^{11}$  copies/g dry sludge at 10 mg/L to  $3.59 \times 10^{11}$  copies/g dry sludge at 40 mg/L.
3. With the increase of  $\text{NO}_3^-$ -N concentration, the quantity and composition of the denitrifying Accumulator IA, Accumulator IIC, Accumulator IIC (*ppk1* excluding OTU NS D3) and Accumulator IID in the branches of phosphorus accumulating bacteria changed significantly. The proportion of Accumulator IIA, IIB and IIF in A/ASBR activated sludge was small, even close to zero, but they were not scoured out of the system.
4.  $\text{NO}_3^-$ -N and variation in concentration affected the number and composition of PAO and its branches in the A/ASBR reactor; thus, it is the main driving factor of the PAO flora structure.

## ACKNOWLEDGEMENT

This work was supported by the National Natural Science Foundation of China (No. 52170034).

## NOMENCLATURE

A/ASBR	: anaerobic/anoxia sequencing batch reactor
ASM2	: activated sludge reaction kinetic model 2
ASM2d	: activated sludge reaction kinetic model 2d
COD	: chemical oxygen demand
DNA	: deoxyribonucleic acid
FISH	: fluorescence in situ hybridization
IWA	: International Water Association
MLSS	: mixed liquor suspended solids
MLVSS	: mixed liquor volatile suspended solids
MUCT	: modified university of cape town
<i>nap</i>	: nitrate reductase gene
<i>nar</i>	: nitrate reductase
<i>nor</i>	: nitric oxide reductase
<i>nos</i>	: nitrous oxide reductase
ORP	: oxidation-reduction potential
PAOs	: polyphosphate accumulating organisms
PCR	: polymerase chain reaction

PHA	: poly- $\beta$ -hydroxy-alkanoates
PHB	: poly- $\beta$ -hydroxy-butyrate
PLC	: programmable logic controller
poly-P	: polyphosphate
ppk	: polyphosphate kinase
qPCR	: real-time fluorescent quantitative PCR
SBR	: sequencing batch reactor
TN	: total nitrogen
TP	: total phosphorus
UCT	: university of cape town
WWTP	: wastewater treatment plant

## REFERENCES

- J. Sargolzaei and A. H. Moghaddam, *Recent Pat. Chem. Eng.*, **6**, 133 (2013).
- T. Zhang, X. S. Wu, S. M. Shaheen, H. Abdelrahman, E. F. Ali, N. S. Bolan, Y. S. Ok, G. X. Li, D. C. W. Tsang and J. Rinklebe, *J. Hazard. Mater.*, **425**, 127906 (2022).
- Y. Yang, H. Q. Zhu, X. H. Xu, L. L. Bao, Y. N. Wang, H. W. Lin and C. Y. Zheng, *Micropor. Mesopor. Mater.*, **324**, 111289 (2021).
- D. D. Ge, H. P. Yuan, J. M. Xiao and N. W. Zhu, *Sci. Total Environ.*, **679**, 298 (2019).
- Q. Guan, G. S. Zeng, J. T. Song, C. L. Liu, Z. B. Wang and S. L. Wu, *J. Environ. Manage.*, **293**, 112961 (2021).
- A. H. Moghaddam and J. Sargolzaei, *J. Disper. Sci. Technol.*, **35**, 563 (2014).
- S. D. A. Masoudi, A. H. Moghaddam, J. Sargolzaei, A. Darroudi and V. Zeynali, *Environ. Prog. Sustain.*, **37**, 1638 (2018).
- A. H. Moghaddam and J. Sargolzaei, *J. Taiwan Inst. Chem. E.*, **49**, 165 (2015).
- M. C. Hascoet and M. Florentz, *Water S. A.*, **11**, 23 (1985).
- A. Gerber, R. H. Villiers, E. S. Mostert and C. J. J. Riet, *The phenomenon of simultaneous phosphate uptake and release and its importance in biological nutrient removal in: Biological phosphate removal from wastewaters*, Pergamon Press, Oxford (1987).
- Y. Comeau, W. K. Oldham and K. J. Hall, *Dynamics of carbon reserves in biological dephosphatation of wastewaters*, Pergamon Press, Oxford (1987).
- K. Øtgaard, M. Christensson, E. Lie, K. Jönsson and T. Welander, *Water Res.*, **31**, 2719 (1997).
- T. Kuba, M. C. M. Van Loosdrecht, F. A. Brandse and J. J. Heijnen, *Water Res.*, **31**, 777 (1997).
- G. J. F. M. Vlekke, Y. Comeau and W. K. Oldham, *Environ. Technol.*, **9**, 791 (1998).
- E. Murnleitern, T. kuba, M. C. M. Van Loosdrecht and J. J. Heijnen, *Biotechnol. Bioeng.*, **54**, 434 (1997).
- J. P. Huang, G. Yan, X. Z. Bian and P. Cheng, *Journal of North China University of Water Resources and Electric Power (Natural Science Edition)*, **42**, 100 (2021) (in Chinese).
- R. L. Xu, Y. B. Fan, Y. S. Wei, Y. W. Wang, N. Luo, M. Yang, X. Yuan and R. Yu, *J. Environ. Sci.*, **48**, 59 (2016).
- T. Kuba, M. C. M. Van Loosdrecht and J. J. Heijnen, *Water Res.*, **30**, 1702 (1996).
- A. Dome, C. Y. Chang, W. Aunnop and P. Chayakorn, *Environ. Technol.*, **42**, 2950 (2020).
- C. Li, S. F. Liu, T. Ma, M. S. Zheng and J. R. Ni, *Chemosphere*, **229**, 132 (2019).
- H. K. Li, Y. M. Zhong, H. Huang, Z. X. Tan, Y. Sun and H. Liu, *Sci. Total Environ.*, **744**, 140852 (2020).
- H. K. Li, H. Liu, Q. Q. Zeng, M. Y. Xu, Y. Y. Li, W. Wang and Y. M. Zhong, *J. Water Process Eng.*, **36**, 101296 (2020).
- V. Zeynali, J. Sargolzaei and A. H. Moghaddam, *Desalin. Water Treat.*, **57**, 24239 (2016).
- J. Sargolzaei, A. H. Moghaddam and J. Shayegan, *Korean J. Chem. Eng.*, **28**, 1889 (2011).
- A. H. Moghaddam, H. Hazrati, J. Sargolzaei and J. Shayegan, *Appl. Water Sci.*, **7**, 2753 (2017).
- A. H. Moghaddam, J. Shayegan and J. Sargolzaei, *J. Taiwan Inst. Chem. E.*, **62**, 150 (2016).
- J. Sargolzaei and A. H. Moghaddam, *Front. Chem. Sci. Eng.*, **7**, 357 (2013).
- H. Mogens, W. Gujer, T. Mino, T. Matsuo, M. C. Wentzel, G. v. R. Marais and M. C. M. Van Loosdrecht, *Water Sci. Technol.*, **39**, 165 (1999).
- J. Londong, *Water Sci. Technol.*, **26**, 1087 (1992).
- E. V. Musvoto, T. G. Casey, G. A. Ekama, M. C. Wentzel and G. V. R. Marais, *The effect of a large anoxic mass fraction and concentrations of nitrate and nitrite in the primary anoxic zones on low F/M filament bulking in nutrient removal activated sludge systems*, Research Report W77, Department of Civil Engineering, University of Cape Town, Rondebosch, 7701, Cape, South Africa (1992).
- X. L. Wang, X. Y. Zhang and H. Lu, *Korean J. Chem. Eng.*, **37**, 249 (2020).
- R. P. Hesselmann, C. Werlen, D. Hahn, J. R. van der Meer and A. J. Zehnder, *Syst. Appl. Microbiol.*, **3**, 454 (1999).
- N. A. Keene, S. R. Reusser, M. J. Scarborough, A. L. Grooms, M. Seib, J. S. Domingo and D. R. Noguera, *Water Res.*, **121**, 72 (2017).
- L. Welles, B. Abbas, D. Y. Sorokin, C. M. Lopez-Vazquez, C. M. Hooijmans, M. C. M. Van Loosdrecht and D. Brdjanovic, *Front. Microbiol.*, **7**, 2121 (2017).
- S. He, D. L. Gall and K. D. McMahon, *Appl. Environ. Microb.*, **73**, 5865 (2007).
- H. G. Martín, N. Ivanova, V. Kunin, F. Warnecke, K. W. Barry, A. C. McHardy, C. Yeates, S. He, A. A. Salamov, E. Szeto, E. Dalin, N. H. Putnam, H. J. Shapiro, J. L. Pangilinan, I. Rigoutsos, N. C. Kyrpides, L. L. Blackall, K. D. McMahon and P. Hugenholtz, *Nat. Biotechnol.*, **24**, 1263 (2006).
- J. J. Flowers, T. A. Cadkin and K. D. McMahon, *Water Res.*, **47**, 7019 (2013).
- M. Albertsen, S. J. McIlroy, M. Stokholm-Bjerregaard, S. M. Karst and P. H. Nielsen, *Front. Microbiol.*, **16**, 1 (2016).
- G. B. Zhu, Y. Z. Peng and S. Y. Wang, *Environ. Eng. Sci.*, **24**, 1111 (2007).
- X. F. Wang, *Method for monitoring and analyzing water and waste water*, China Environmental Science Press, Beijing (2002).
- C. Li, *Population dynamics and morphotypes analysis of paos in denitrifying phosphorus removal systems*, Beijing University of Technology, Beijing (2018).
- B. X. Li, *Study on function and community structure of candidatus accumulibacter in denitrifying phosphorus removal system*, Beijing University of Technology, Beijing (2013).

43. Y. P. Mao, D. W. Graham, H. Tamaki and T. Zhang, *Sci. Rep.*, **46**, 11857 (2015).
44. Z. R. Hu, M. C. Wentzel and G. A. Ekama, *Water Res.*, **36**, 4927 (2002).
45. W. Zeng, X. L. Bai, Y. Guo, N. Li and Y. Z. Peng, *Enzyme Microb. Tech.*, **105**, 1 (2017).
46. W. Zeng, B. X. Li, X. D. Wang, X. L. Bai and Y. Z. Peng, *Chemosphere*, **144**, 1018 (2016).
47. P. Y. Camejo, B. R. Owen, J. Martirano, J. Ma, V. Kapoor, J. S. Domingo, K. D. McMahon and D. R. Noguera, *Water Res.*, **102**, 125 (2016).
48. C. T. Skennerton, J. J. Barr, F. R. Slater, P. L. Bond and G. W. Tyson, *Environ. Microbiol.*, **17**, 1574 (2015).
49. J. J. Flowers, S. He, S. Yilmaz, D. R. Noguera and K. D. McMahon, *Env. Microbiol. Rep.*, **1**, 583 (2009).
50. G. Carvalho, P. C. Lemos, A. Oehmen and M. A. M. Reis, *Water Res.*, **41**, 4383 (2007).